

Military Comparison of 3D Printed Vs Commercial Components

Janice Booth,^a Eugene Edwards,^a Michael Whitley,^b Michael Kranz,^b Mohamed Seif,^c Paul Ruffin^c

^aU. S. Army Research, Development, and Engineering Command
Redstone Arsenal, Alabama 35898
E-mail: usarmy.redstone.rdecom-amrdec.mbx.pao@mail.mil
Phone: 256-842-2142

^bEngeniusMicro, Huntsville, Alabama 35801

^cAlabama A&M University, Normal, Alabama 35762

ABSTRACT

The Army continues the development of 3D printing technology to enhance the capability to produce smaller and lighter precision weaponry. Researchers and support organizations that are affiliated with the Army Aviation and Missile Research, Development, and Engineering Center (AMRDEC) are developing nano-based structures and components for advanced weaponry, aviation, and autonomous air/ground systems applications. The first key area consists of determining in-plane and out-of-plane shear properties of test articles made by 3D printing (Fused Deposition Modeling - FDM) and comparing to the conventional extrusion/forming sheet process. Test specimens are made from three polymer materials: acrylonitrile butadiene styrene (ABS), high impact poly-styrene (HIPS), and poly-lactic acid (PLA). Laboratory testing is performed according to the ASTM D3846-02 method for determining the in-plane shear strength, while the ASTM D5379 method is used for determining the out-of-plane shear properties. A description on how the 3D printing process advances the shear properties and has the potential of improving the in-plane and cross-sectional shear properties over the conventional manufacturing process is presented. The second key area demonstrates a set of materials, processes, and techniques that support the enabling of additive manufacture (AM) of RF components. Research activities are focused on developing open-source hardware/software multi-material direct digital printing, and producing 3D printed antenna, passive components, and connectors for C-band and Ku-band systems. Material studies have demonstrated a suitable material set for RF components and identified key material performance limits. Results show how more enhancement could be achieved by optimizing the variables that affect 3D printing.

Keywords: nano-based precision weaponry, fused deposition modeling, components shear properties, 3D printing, additive manufacturing, direct digital printing, open-source hardware, and RF components

This information product is approved for public release. The views and opinions of its authors do not necessarily state or reflect those of the U.S. Government or any agency thereof. Reference to any specific commercial product, process, or service by trade name, trademark, manufacturer, or otherwise does not necessarily constitute or imply its endorsement, recommendation, or favoring by the U.S. Government or any agency thereof."

1. INTRODUCTION

During the past decade, the US Army Aviation and Missile Research, Development, & Engineering Center (AMRDEC) has continuously researched the areas of innovative smart micro-sensors, nano-based materials, nano devices, nano-based sensors, remote readiness prognostics, and structural health monitoring [1-6]. The Army AMRDEC has likewise become very interested in and continues to investigate methods associated with 3D printing for direct manufacturing of antennas, interconnects, printed circuit boards, sensors and other devices [7]. It is common knowledge that 3D electronics printing is an emerging technology that is poised for more growth as an innovative additive manufacturing methodology. One of the many items of particular interest to Army AMRDEC is state-of-the-art 3D printing approaches for rapid prototyping of antennas, along with results from the comparison of standard manufactured antenna prototypes to its 3D printed reproduction. Several research establishments have outlined work associated with the 3D printing of antenna. Such research included rapid prototyping of electrically small spherical wire antennas [8]; 3D printing electrically small spherical antennas [9]; and compact form fitting small antennas using three-dimensional rapid prototyping [10].

Selected capabilities, in terms of rapid 3D printing components (such as embedded sensors, actuators, and compact systems), have been researched by the Army. The Army AMRDEC has investigated research conducted by various universities and national laboratories relative to technology that includes stretchable material in the 3D printing process of the structure for form-fitting objects that are amenable for wearable applications [11]. Research of interest includes the development of smart physical assisting and therapeutic wearable device. These devices were personalized and tailored to patient's condition and body for thermotherapy (where application of heat at the point of injury is required to enhance blood flow and reduce pain) [12].

Over the recent years, additive manufacturing has been used as a viable alternative manufacturing methodology. Efforts currently underway to assess additive manufacturing for military applications are discussed in this paper. During the past several years, the US Army AMRDEC initiated research and development programs that include a program called "PRIntable Materials with embedded Electronics (PRIME2)." The objective of the PRIME2 program was to develop new fabrication capabilities that integrate Radio Frequency (RF) and electronic components into additive manufacturing processes. The overall goal is to reduce the size, weight, and overall cost of weaponry components and subsystems. A primary objective for the project is to utilize a one-step process to print an entire printed wiring board with embedded passive components and integrated RF structures [13]. An initial task involves the use of additive manufacturing techniques to develop, simulate, and test a planar monopole antenna [14]. Previously conducted studies were continued that utilized varying manufacturing processes (i.e., 3D Printing and conventional methods, such as standard Extrusion/Forming Methods). The goal of the research is to conduct additional assessments of the achievability of additive manufacturing for military applications [14, 15]. Various laboratory artefacts were prepared using several materials that were tested for mechanical strength. Results from the research are being used to evaluate the feasibility of the additive manufacturing process for military applications. Outcomes from these investigations are presented and discussed in this manuscript.

As in previous work, the Army can use the results to revolutionize existing (and future) weaponry systems by significantly reducing the size, weight, and cost. One example of such use could be to support the development and characterization of low cost seeker technology for varying applications. Such developments may support the Army Research Laboratory's exploration of seeker technologies for use with guided munitions as part of the Army Technology Objective's (ATO's) appeal for Smaller, Lighter, and Cheaper Munition Components (SLCMC). Such efforts may include the ARL/ATO/SLCMC desire for a semi-active laser (SAL) seeker hardware utilizing electronic components that may be created via alternative manufacturing methodologies. The SAL seeker provides a terminal homing capability based on laser energy reflected for the target [16]. The research in this paper will reveal the concepts, findings/results, and conclusions associated with alternative manufacturing (i.e., 3D printing) of electronics components/antennas.

2. COMPARISON OF 3D PRINTED PLASTIC SHEETS VS EXTRUSION SHEETS

The laboratory methodology concentrates on determining the in-plane and out-of-plane shear properties of test articles made by the 3D printing process (Fused Deposition Modeling - FDM) and the conventional extrusion/forming sheet process. Test specimens were made from three polymer materials: Acrylonitrile Butadiene Styrene (ABS), High Impact Poly-Styrene (HIPS), and Poly-Lactic Acid (PLA). The testing procedures were performed according to the American Society for Testing and Materials (ASTM) method (i.e., ASTM D3846–02) for defining the in-plane shear strength while the ASTM D5379 method has been used for determining the out-of-plan shear properties. Hence, the specimen dimensions, testing method and procedures, loading jig configuration, tightening torque and other recommendations are used based on the standards mentioned above. For in-plane shear tests, failure of the specimen occurs in shear between two centrally located notches machined halfway through its thickness and spaced a fixed distance apart on opposing faces. Next, the standard test method for shear properties by the V-Notched Beam Method is adopted to determine the cross-sectional (out-of-plane) shear strength. In this condition, the shear strength is defined as the structural failure yield at rupture in which the plane of fracture is located perpendicular to the longitudinal axis of the specimen and between the two centrally located V-Notches.

The test results of the in-plane and cross-sectional shear tests for the ABS, HIPS, and PLA materials show that the 3D printing process advances the shear properties and has the potential of improving the in-plane shear and cross-sectional shear properties over the conventional manufacturing process. Moreover, this study shows that more enhancement could be achieved by optimizing the effect of the different variables that affect the 3D printing process. These variables would be the bed temperature, the chamber temperature, the nozzle diameter, layer thickness, melt pool temperature, and the cooling rate.

It should be noted that the coefficient of variance in this investigation of any tested material has never exceeded 5% with an average of 2.25%. Hence, the 3D printer process provides reliable and compatible products compared with the conventional extrusion/forming process, yet with two main advantages: 1) making complex parts and 2) higher shear stresses.

Figure 1 shows the embodiment of the additive manufacturing process. The process includes the laser melting stage; laser polymerization stage; thermal extrusion stage; material jetting stage; material adhesion stage; and electron beam. The laser melting uses the laser beam to melt and fuse the metal powders together [17]. The electron beam melting process is similar to the laser melting process except it works on layer by layer methodology and uses process parameters such as beam power, beam scanning velocity, beam focus beam diameter, beam line spacing, plate temperature, pre-heat temperature, contour strategies, and scan strategies [18].

Additive Manufacturing (AM) Processes										
Process	Laser Based AM Processes				Extrusion Thermal	Material Jetting	Material Adhesion	Electron Beam		
	Laser Melting		Laser Polymerization							
Process Schematic										
Name Material	SLS	DMD	SLA	FDM	3DP	LOM	EBM			
	SLM	LENS	SGC	Robocasting	IJP	SFP				
	DMLS	SLC	LTP		MJM					
		LPD	BIS		BPM					
			HIS		Thermojet					
Bulk Material Type		Powder	Liquid	Solid						

Figure 1. Embodiment of the additive manufacturing process

In Table 1 below, additive manufacturing techniques and basic elements are outlined. The table shows the monitored additive manufacturing attributes for each of the processes to the left. For instance, laser polymerization has the monitored attributes of laser power/distribution, chamber temperature, chamber vacuum, platform position, and head position.

Table 1 Additive Manufacturing Techniques and Basic Elements

ADDITIVE MAMUFACTURINS TECHNIQUES & BASIC ELEM ENTS									
Am Process	Monitored Attribute								
	Laser Power/ Distribution	Melt Pool Temperature	Nozzle Temperature	Jet Status	Chamber Temperature	Chamber Vacuullm	Platform Position	Head Position	
Laser Polymerization Process	X				X	X	X	X	
Laser Melting Process	X	X			X	X	X	X	
Extrusion Process		X	X		X		X	X	
Material Jetting Processes				X	X		X	X	
Adhesive Processes					X		X	X	

Figure 2 illustrates the modeling approach relative to fused deposition modeling (FDM) associated with the extrusion process. In a typical fused deposition modeling extrusion additive manufacturing process, the filament material is supplied into the extrusion zone and melted in a heated liquefier. Typical systems utilize a thermocouple to measure consistent heating element temperature and a controller to maintain a constant temperature [19]. The un-melted portion of the filament acts as a piston that pushes the melted portion through the print nozzle. The overall process allows for 3D objectives to be manufactured as the melted filament material from the nozzle becomes solid. It is common knowledge that the most common filament material is amorphous thermoplastics, e.g., acrylonitrile butadiene (ABS).

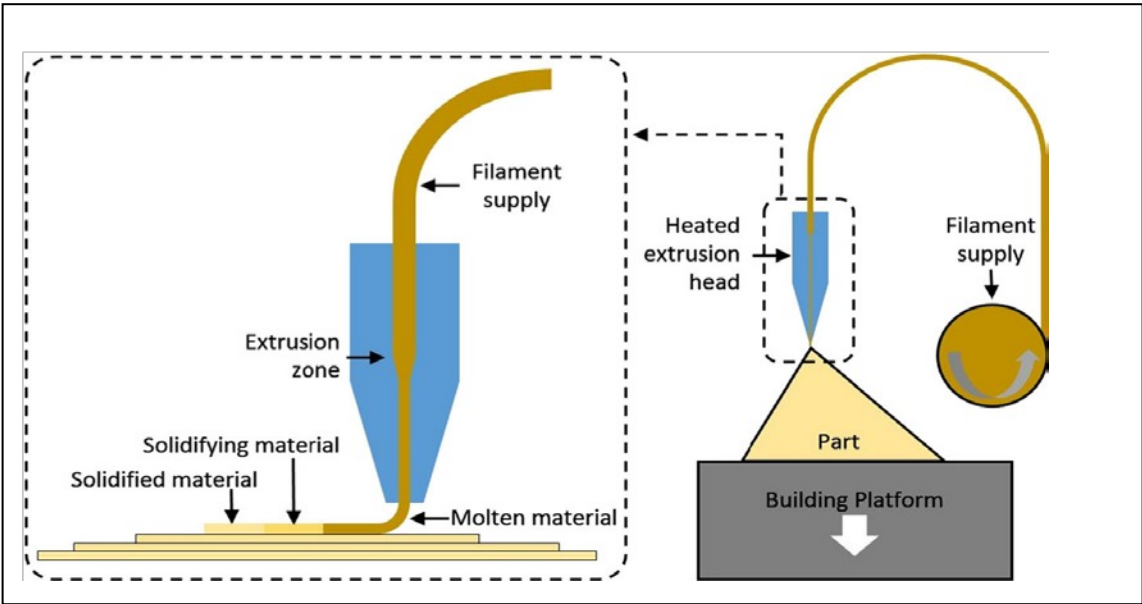


Figure 2. Modeling Approach Associated with the Extrusion Process

More details of the extrusion process, including the sectional view of the five zones of the melt flow channel, are shown in Figure 3. For most of the typical melt extrusion additive manufacturing configurations, key design parameters include the liquefier length, liquefier/filament diameter, nozzle angle (typically 200-500 micrometers nozzle diameter at angles of approximately 120 degrees) [20].

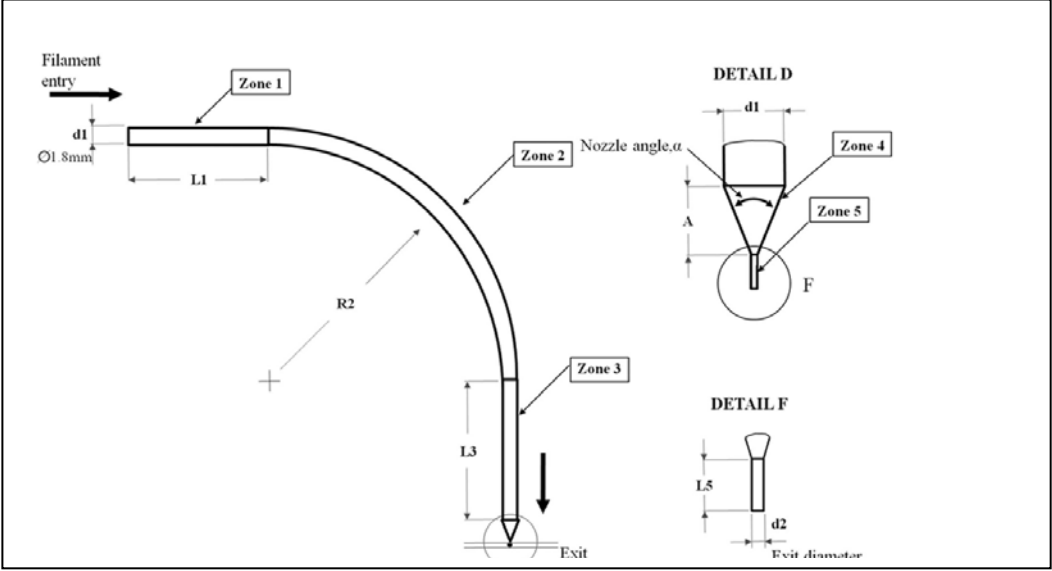
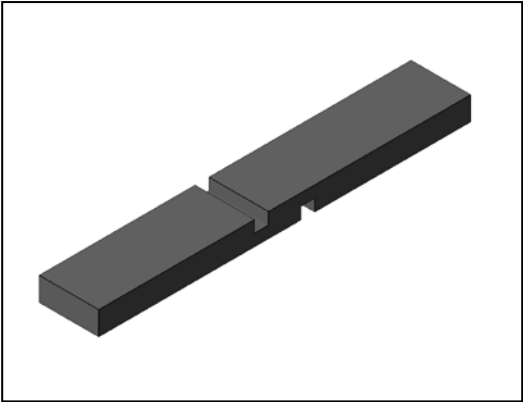
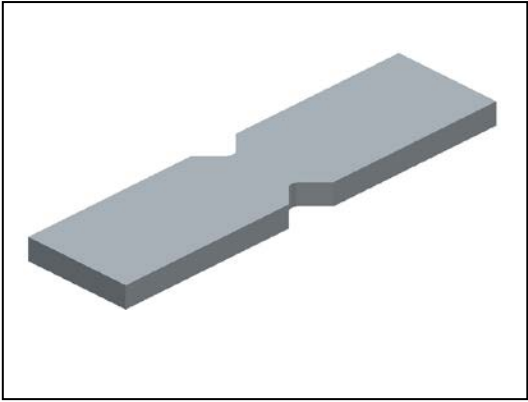


Figure 3. Sectional view of the five zones of the filament melt flow channel

Laboratory/experimental apparatuses and methodologies were implemented to test mechanical elements of varying shapes of test specimens in order to determine the consistency of the mechanical strength of each shape. As depicted in Figure 4, in-plane shear test specimens were fabricated (and evaluated per ASTM D3846 test methods), along with the fabrication of V-notch test specimens (evaluated per ASTM D5379 test methods). It is common knowledge in the reinforced plastics industry (per ASTM D3846) that shear testing is used to assess the strength of the reinforcement-to-resin bond in polyester-, vinyl ester-, and epoxy-resin composites. On the other hand and per ASTM D5379, the V-notched beam test method gives strength via shear properties of composite materials reinforced by high-modulus fibers.



(a) In-Plane Shear Specimen for ASTM D3846 method



(b) V-Notch Specimen for ASTM D5379 method

Figure 4. Test specimens and methods (note: D1892 standard has been used for Extrusion/Forming sheet process)

The specimens were fabricated from acrylonitrile butadiene styrene (ABS), high impact poly-styrene (HIPS), and poly-lactic acid (PLA, a bio-plastic) thermoplastic materials. The two autonomous methods used to fabricate the specimens were fused deposition modeling (FDM) 3D printing (per the recommendation of the 3D printer manufacturer) and conventional extrusion forming (CEF) sheet processing (the specimens are cut from sheets of the chosen plastics and prepared per ASTM D1892 standards).

As part of the Army AMRDEC's continued interest in the development of the printed 3D antennas (and subsequently other electronic devices), the mechanical stability of printed specimens is valuable. In order to understand the changes in the mechanical properties of the printed specimens, comparative studies were performed. The mechanical changes in strength are obviously related to choices of material and printing techniques.

In prior studies, a single FDM 3D printing process is compared to a traditional subtractive manufacturing process utilizing the previously mentioned ASTM standards as guides. Much of the same previous efforts is done and now repeated by way of the fabrication of standardized mechanical test coupons that are then subjected to mechanical testing. Conventional material extrusion and machining are the traditional processes employed. Previous efforts utilized test specimens made from ABS, HIPS, and PLA polymer materials. Each test specimen was subjected to standardize mechanical in-plane shear and V-notched beam test methods previously outlined in this paper and shear properties by V-Notched rail shear method per (ASTM D7078). The efforts were conducted in the manner as recommended in the cited standards and the specimen's dimensions, testing method/procedures, loading jig configuration, tightening torque, and other recommendations were all based on the standards.

The test specimen is shown in the test jig of Figure 5 (below) before and after being compressive loaded. In-plane shear strength is defined as the structural failure yield at rupture in which the plane of fracture is located along the longitudinal axis of the specimen between two centrally located notches that are machined halfway through the specimen's thickness on opposing faces [7]. The test specimen is mounted edgewise in the support jig and the assembly is then placed in the compression testing machine. A compressive load is applied to the notched specimen at a specified rate in order to determine the in-plane shear strength. The maximum load (at the moment of rupture) carried by the specimen during the test is recorded. Failure of the specimen occurs in shear between the two centrally located notches machined halfway through the specimen's thickness and spaced a fixed distance apart on opposing faces.

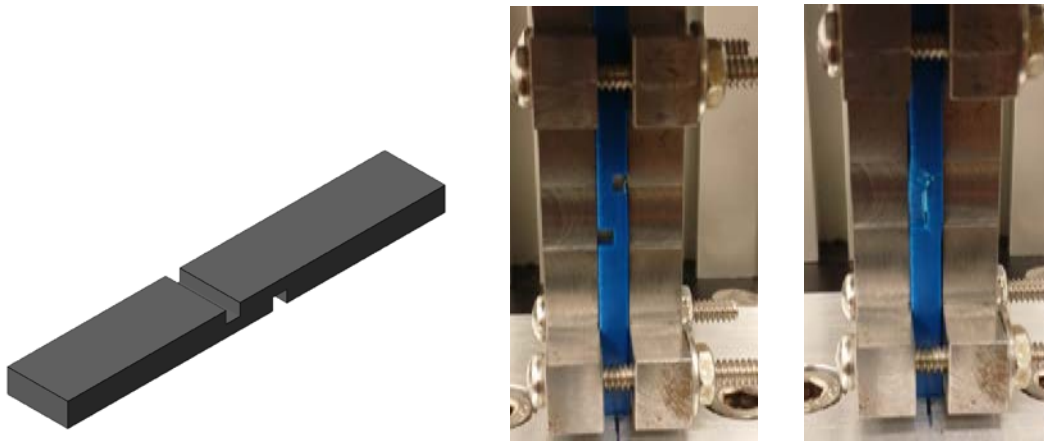


Figure 5. (left) In-plane shear strength test specimen; (middle) specimen mounted in test jig; and (right) specimen after mechanical failure

The standard test method for shear properties of composite materials (by the V-Notched beam method) is now adopted and outlined as used to determine the cross-sectional shear strength. The test specimen is shown mounted and

tested in Figure 6 (below). Shear strength is defined as the shear strength at rupture in which the plane of fracture is located perpendicular to the longitudinal axis of the specimen and between the two centrally located V-Notches [7]. The specimen is mounted in the supporting jig and the assembly is then placed in the compression test machine (which has both a stationary and a moving head). A compressive load is applied to the V-notched specimen at a specified strain rate to determine the cross-sectional shear strength. The maximum load (at the moment of rupture) carried by the specimen during the test is recorded. Failure of the specimen occurs in shear between the two centrally located V-notches machined at the center of the specimen.

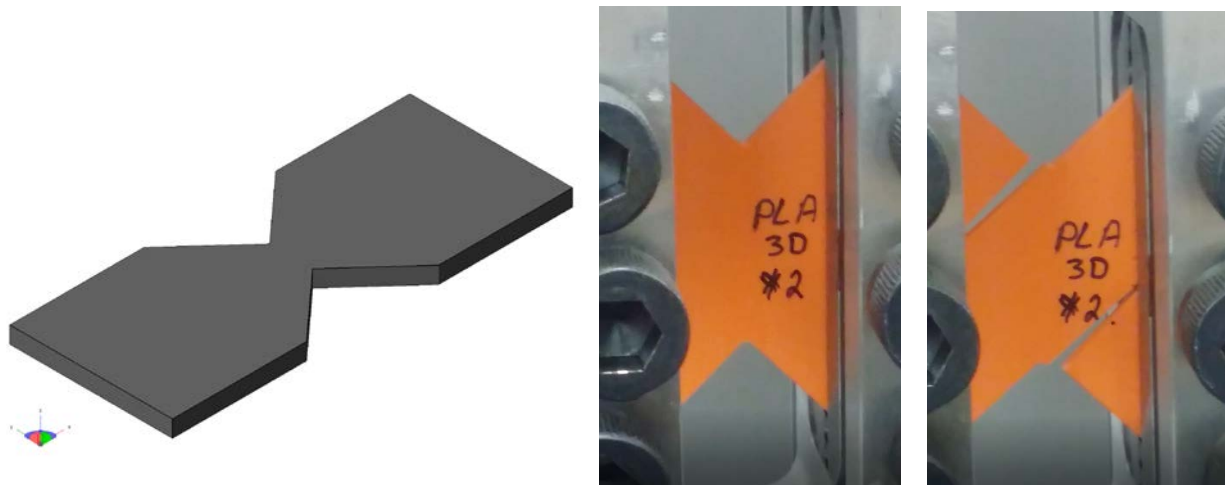


Figure 6. (left) Shear properties test specimen; (middle) specimen mounted in test jig; (right) specimen after mechanical failure

Test results are documented here and the outcomes are identifiable. The results from the in-plane and cross-sectional shear tests for the ABS and HIPS materials are shown in Figures 7 and 8 (below). Results show that the 3D printing process comparatively improves the in-plane shear and cross-sectional shear properties over the conventional manufacturing process. Moreover, this study shows that more enhancements could be achieved by optimizing the effect of the assortment of variables that affect the 3D printing process. These variables consist of the bed temperature, chamber temperature, nozzle diameter, layer thickness, and melt pool temperature.

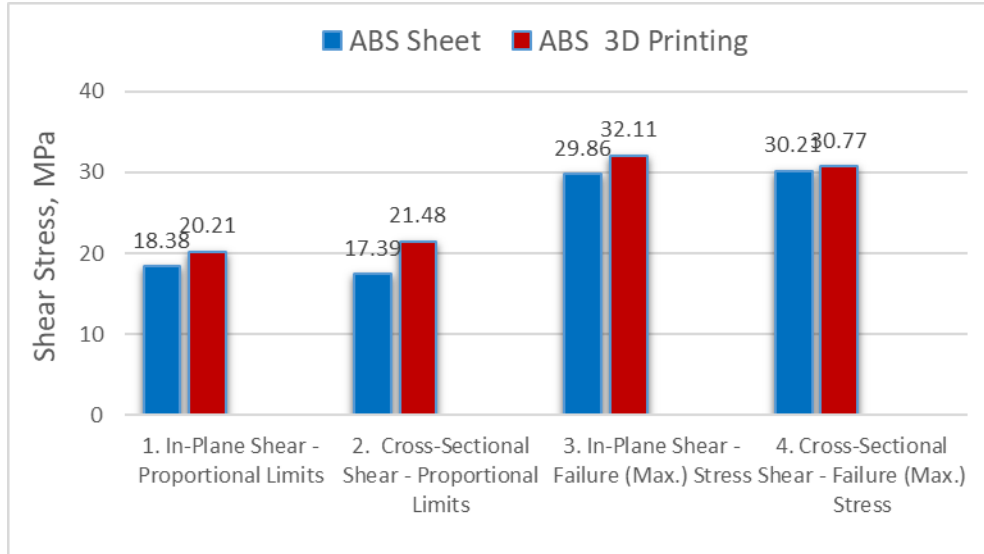


Figure 7. (In-plane and cross-sectional shear stress results for ABS filament)

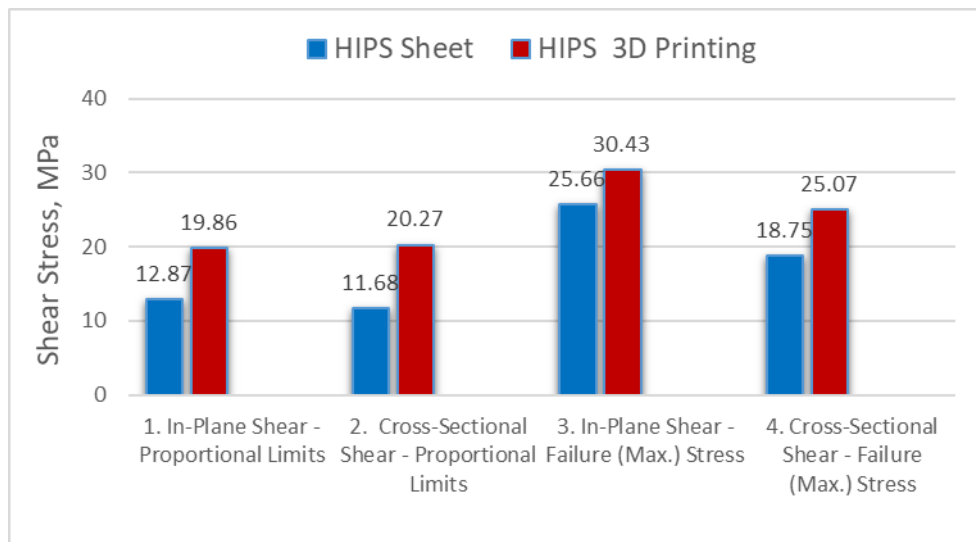


Figure 8. In-plane and cross-sectional shear stress results for HIPS material

3. COMPARISION OF 3D PRINTED ANTENNAS VS STANDARD ANTENNAS

The conventional method for manufacturing RF structures and electronic components involves piecemeal assembly techniques. This method is time consuming and has drawbacks (e. g., lossy structures (antennas)) that are inherent in the manufacturing process for fabricating antenna elements, RF structures, and connections. Additive manufacturing is a promising capability with a plethora of potential benefits, including the reduction of complexity, elimination of the requirement to assembly parts, and other advantages. The US Army AMRDEC initiated the PRIME2 program (previously described above in this paper) to investigate the feasibility of using additive manufacturing processes to print antenna elements, RF structures, and connections. There are current efforts to support efforts to examine the capabilities and limitations of additive manufacturing for military applications. Initially, a planar monopole antenna was fabricated using 3D printing to assess the feasibility of integrating RF structures and electronic components relative to the additive manufacturing process. The viability of 3D printing for military applications is subsequently evaluated by conducting a comparative study implementing two different manufacturing processes and the use of three different materials that are currently employed in 3D printing. Results from the ongoing fabrication of antennas, associated with the use of 3D printing techniques for military applications, are discussed in this section.

Multiple 3D printers were used to fabricate a planar, S-band inverted F monopole antenna in an attempt to understand potential issues associated with the implementation of electronic components and RF structures produced via additive manufacturing. Hand-solder techniques and conductive epoxy techniques were used to connectorize the antennas to a standard sub-miniature version A (SMA) connector. The first version of the printed antennas was tested in the AMRDEC RF Technology Function's clean room at Redstone Arsenal (Alabama). Conventional simulation techniques were used to obtain theoretical antenna patterns, 3D and Two-Dimensional (2D) cuts, and S11 results (S-Parameter that represents the amount of power reflected from the antenna). The results predict that the antennas would radiate well within the range of antennas fabricated using conventional manufacturing processes (see Figure 9, below).

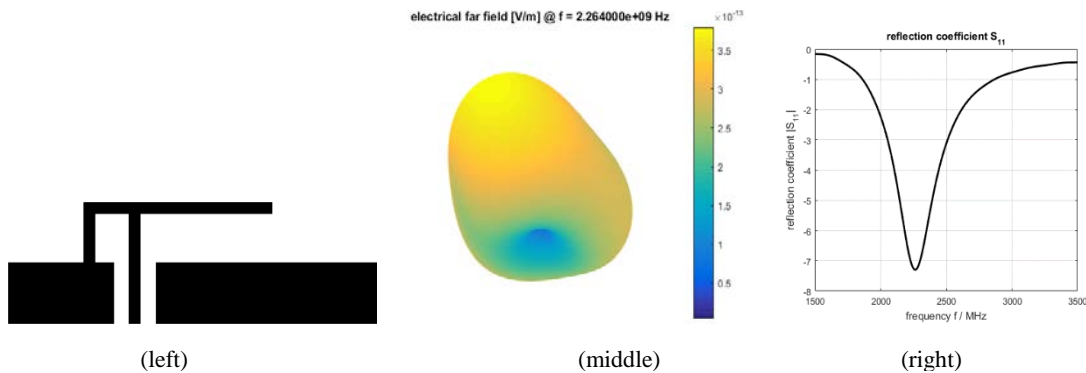


Figure 9. (left) Planar Inverted F Antenna Geometry; (middle) simulated 3D far field radiation pattern; (right) simulated reflection coefficient

The planar S-Band inverted F monopole was first printed using nanoparticle silver ink on a Dimatrix DMP-2831 inkjet multi-material printer on a simple non-conductive paper substrate. The printer and antenna on flexible paper substrate are shown below in Figure 10.

After printing, and in order to form a continuous conductive film, the ink was sintered at an elevated temperature of 110 degrees C. The nanoscale nature of the ink leads to high surface energies that allow sintering at temperatures significantly lower than the melting temperature of the base material. The antenna was subsequently cut out of paper substrate and a SMA connector was soldered to the antenna using a low-temperature soldering technique coupled with high silver content solder.



Figure 10. (left) Dimatix DMP-2831 Inkjet Printer and (right) Connectorized Planar Inverted F Nanoparticle Silver Antenna on Flexible Paper Substrate

A Voxel8 printer was used to print a similar antenna structure. This print incorporated room temperature-cured silver nanoparticle epoxy as the conductor and poly-lactic acid as the dielectric substrate. The antenna was designed to operate at 2GHz. An SMA connector was attached to the antenna using a high conductivity two-part room temperature-cured conductive epoxy. The completed antenna (in Figure 11, below) was coupled to a network analyzer using a 50 ohm coaxial cable; the S-parameters were captured. The antenna demonstrates good matching and bandwidth at the expected frequency.

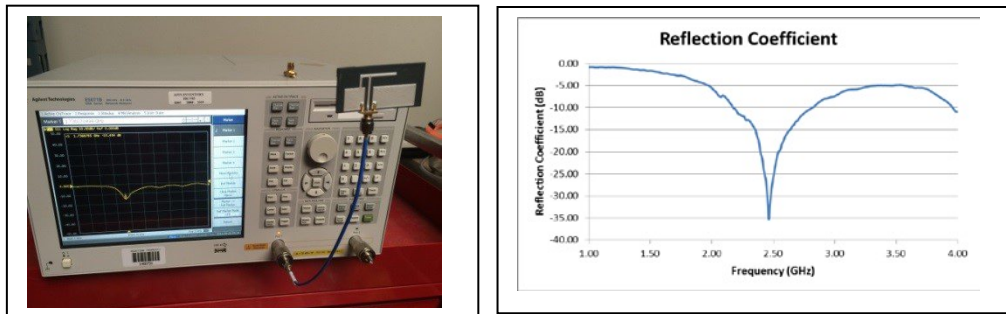


Figure 11. (left) Connectorized 3D printed inverted f antenna being tested on a vector network analyzer and (right) reflection coefficient as a function of frequencies demonstrates good matching and bandwidth

In the next phase of the research, efforts were made to correspondingly demonstrate a set of materials, processes, and techniques utilizing additive manufacture (AM) to fabricate RF components. Activities focused on developing open-source hardware/software multi-material direct digital printing; and producing 3D printed antenna, passive components, and connectors for C-band and Ku-band systems. Material studies were conducted where samples were printed and electrical parameters (including permittivity, losses, and operating temperatures) were measured for 35 printable dielectrics. The material study also investigated 5 printable conductors and measured conductivities as high as 30% of bulk silver with printed silver nanoparticles. The material study demonstrated a suitable material set for RF components and identified key material performance limits. The material and process studies were applied to a series of prototypes to demonstrate 3D printed C-band and Ku-band antennas, baluns, power splitters, feed lines, and connectors. The fabrication of RF connectors provided unique challenges for the 3D printing processes because they are highly 3D in nature and often incorporate screw threads, small pins, high tolerances, and rotating pieces. Additionally, they undergo significant mechanical stresses during mating and de-mating. In order to accommodate these requirements, stereolithographic approaches were combined with electroplating to achieve high resolution robust 3D structures. More than 20 complete SMA connectors were fabricated and underwent mechanical testing by mating with off the shelf SMA

connectors. This suite of prototypes demonstrates the ability to apply additive manufacturing and 3D printing to a broad range of RF components. The suite demonstrates a command of material integration, process modification, and hardware modification which will serve to further improve performance and reliability in the next development cycle. A key objective is to create RF structures (including antennas) using low cost additive manufacturing technologies.

Typical equipment used in the 3D printing process included the Dimatix DMP-2831 Inkjet multi-material printer, fused filament process (Taz Luzbot layers and/or Franken Taz strands); and multi-material (Voxel8 developer's kit and/or EngeniusMicro dispense). Examples are shown below in Figure 12. Volumetric 3D printed parts (with embedded circuits and components) can be created with the Voxel8 developer's kit. Preliminary substrate and insulation layers were fabricated from the common and popular acrylonitrile butadiene styrene (ABS) plastic.



Figure 12. (left) Dimatix DMP-2831 Inkjet multi-material printer; (center) LulzBot TAZ 6 3D Printer; and (right) Voxel8 developer's kit

In the laboratory, the best of each printer's capabilities were used (Figure 13); the necessary workpiece transfers were made; and a finished item/cured assembly was realized.

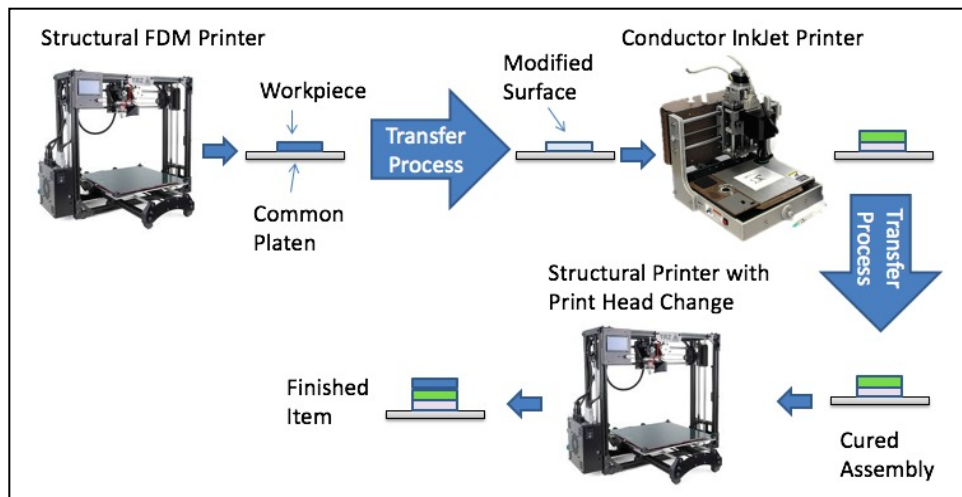


Figure 13. Best of each printer's capabilities utilized to fabricate finished item/cured assembly

The key approach to this research was to design rudimentary RF elements and antennas such that the building blocks of an RF front end could be tested (including a microstrip transmission line, antenna, and power splitter). Expectations are for these additive manufactured technologies to provide low profile, low-cost, flexible electronics and other RF elements. Additive manufactured printed transmission lines are expected to be fabricated in a relatively simple and economical manner. Resulting printed transmission lines should be less susceptible to fracturing when compared to traditional commercially manufactured transmission lines.

In left portion of Figure 14 below, a laboratory fabricated additively manufactured SMA connector is attached to the left end of a commercially fabricated microstrip transmission line. The entire fixture was compared to an equivalent commercially fabricated microstrip transmission line (top portion of the figure) with commercial connectors on both ends. The characteristic impedance is 46 ohms and a loss of 13db/m. The graph on the right side of Figure 14 is the comparison of the transmission line (TX) input reflection coefficient parameter (S_{11} , with the output of the network terminated by a matched load) characteristics for the line with the additively manufactured SMA connector versus the line with commercial connectors on both ends. Results are quite favorable.

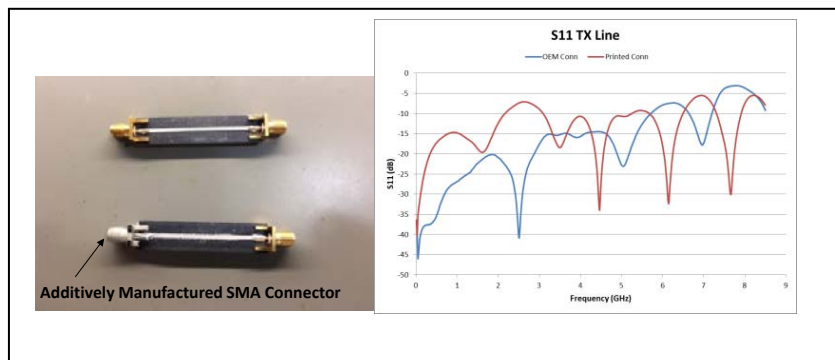


Figure 14. (left) 3D printed SMA connector connected to left end of commercial microstrip transmission line and compared to totally fabricated line shown at the top; (right) graphical reflection parameter, S_{11} comparison

Relative to recent 3D printed antennas, one of the antennas fabricated in the laboratory is shown below in Figure 15. The figure shows the conceptual diagram of the Ku-Band microstrip-fed patch antenna, along with the actual Ku-Band antenna, and the S_{11} characteristics of the Ku-Band microstrip-fed patch antenna. The approximate -18 dB S_{11} reflection characteristic at approximately 16.5 Ghz is quite respectable.



Figure 15. (left) Conceptual diagram of Ku-Band microstrip-fed patch antenna; (middle) actual Ku-Band antenna; (right) S_{11} characteristics of the Ku-Band microstrip-fed patch antenna

4. CONCLUSION

Results from the Army AMRDEC's research and development of contemporary fabrication capabilities for the integration of radio frequency (RF) and electronics components/subsystems into additive manufacturing processes have been outlined in this paper. Expectations are for the generation of enhanced methodologies to reduce size, weight, and overall cost of components for military applications.

In-plane and out-of-plane shear properties of test articles, made by 3D printing (Fused Deposition Modeling - FDM), were generated and compared to conventional extrusion/forming sheet fabricated test articles. Test specimens were made from three polymer materials: acrylonitrile butadiene styrene (ABS), high impact poly-styrene (HIPS), and poly-lactic acid (PLA). Laboratory testing was successfully performed according to the ASTM D3846-02 method for determining the in-plane shear strength, while the ASTM D5379 method was used to determine the out-of-plane shear properties. Description of the 3D printing process ability to advance the shear properties was outlined and the potential for improving the in-plane and cross-sectional shear properties over the conventional manufacturing process was presented.

In the second part of the research, a set of materials, processes, and techniques that support the enabling of additive manufacture (AM) of RF components were demonstrated. Research activities were focused on developing open-source hardware/software multi-material direct digital printing and producing 3D printed antenna, passive components, and connectors for C-band and/or Ku-band systems. Others in the open literature have successfully demonstrated and characterized fully 3D printed RF structures [21]. Material studies in this paper demonstrated that a suitable material was set for RF components, along with the identification of key material performance limits. Results show that additional enhancements could be achieved by optimizing the variables that affect 3D printing.

REFERENCES

- [1] Ruffin, P. B., Brantley, C. L. and Edwards, E., “Innovative smart microsensors for Army weaponry applications,” Proc. SPIE 6931, 6931-1 (Mar. 2008).
- [2] Ruffin, P. B., Brantley, C. L. and Edwards, E., and Mensah, T., “Nano-based materials for use in missile.” AIAA Conference (Mar. 2012).
- [3] Edwards, E., Brantley, C. L., and Ruffin, P. B., “Nano devices and concepts for condition-based maintenance of military systems,” Proc. SPIE 9434, 9434-02 (Apr. 2015).
- [4] Brantley, C. L., Edwards, E., and Ruffin, P. B., “Nano-based sensor for weaponry structural degradation,” Proc. SPIE 9802, 9802-02 (Apr. 2016).
- [5] Marotta, S.A., “Remote readiness asset prognostic and diagnostic system (RRAPDS)”, JANNAF Health Management And Reliable Service Life Prediction, Hill AFB, Ogden, Utah, (Oct. 2004).
- [6] Marotta, S.A., Ooi, T.K., Gilbert, J.A., “Structural health monitoring of strategically tuned absolutely resilient structures (Stars),” Proc. Of Sem X International Congress, Costa Mesa, California, Paper No. 172, (Jun. 2004).
- [7] Edwards, E., Booth, J. C., Roberts, J. K., Brantley, C. L., Crutcher, S. H., Whitley, M., Kranz, M., Seif, M., and Ruffin, P. B., “Military efforts in nanosensors, 3D printing, and imaging detection,” Proc. SPIE 10167, 10167-14 (Apr. 2017).
- [8] Kim, O.S., “Rapid prototyping of electrically small spherical wire antennas,” IEEE Trans Antennas 62, pp. 3839-3842 (Jul. 2014).
- [9] Kim, O.S., “3D printing electrically small spherical antennas,” IEEE Antennas Propagation Society International Symposium 2013, pp. 776-777 (Jan. 2014).
- [10] Willis, B.J., “Compact form fitting small antennas using three-dimensional rapid prototyping,” University of Utah ProQuest Dissertations & Theses – Thesis # AAT 3505035/ISBN: 9781267289155, vol. 73-08(E) (May. 2012).
- [11] Ota, H., Emaminejad, S., Gao, Y., Zhao, A., Wu, E., Challa, S., et. al., “Application of 3D printing for smart objects with embedded electronic sensors and systems,” Advanced Material Technologies, Weinheim, Germany, Volume 1, Issue 1, 1600013, (Apr. 2016).
- [12] Michlovitz, S., Hun, L., Erasala, G.N., Hengehold, D.A., Weingand, K.W., , “Continuous low-level heat wrap therapy is effective for treating wrist pain,” Arch. Phys. Med. Rehabil., Weinheim, Germany, Volume 85, Issue 9, 1409-1416, (Sep. 2004).
- [13] Booth, J., LeFevre, V., Whitley, M., and Kranz, M., “A Planar S-Band Inverted F Monopole Antenna Created Using Additive Manufacturing,” TR-RDMR-WD-16-22, United States (U.S.) Army Aviation and Missile Research, Development, and Engineering Center (AMRDEC), Redstone Arsenal, AL, (Apr. 2016)
- [14] Booth, J., Whitley, M., Kranz, M., Seif, M., and Ruffin, P., “A Comparative Study Between 3D Printing and Forming Processes Using In-Plane Shear Strength Testing of ABS, HIPS, and PLA Plastics,” TR-RDMR-WD-16-43, United States (U.S.) Army Aviation and Missile Research, Development, and Engineering Center (AMRDEC), Redstone Arsenal, AL, (Jul. 2016)
- [15] Booth, J., Whitley, M., Killen, L., Rudd, C., and Kranz, M., “Printable Materials with Embedded Electronics (PRIME2), Break Analysis for Printed Materials,” TR-RDMR-WD-16-58, United States (U.S.) Army Aviation and Missile Research, Development, and Engineering Center (AMRDEC), Redstone Arsenal, AL, (Nov. 2016)

[16] Barth, J., Fendt, A., Florian, R., Kieslich, W., "Dual Mode Seeker with Imaging Sensor and Semi-Active Laser Detector," Proc. SPIE 6542, 6542-B (May. 2007).

[17] Herzog, D., Seyda, V., Wycisk, E., Emmelmann, C., "Additive Manufacturing of Metals," Acta Material 2016;117:371-392. Doi:10.1016/j.actamat.2016.07.019. (Jun. 2017)

[18] Arcam EBM (GE Additive Company) Electron Beam Melting of Metals. [(accessed 19 February 2018)]; Available online:, <http://www.arcam.com/technology/electron-beam-melting/materials/>. (Jun. 2017)

[19] Gibson, I., Rosen, D.W., Stucker, B., "Additive Manufacturing Technologies: Rapid Prototyping to Direct Manufacturing," Springer, New York, New York, (Nov. 2014).

[20] Yardimci, M.A., Hattori, T., Guceri, S.I., Danforth, S.C., "Thermal Analysis of Fused Deposition," in Bourell, D.L., Beaman, J.J., Crawford, R.H., Marcus, H.L., Barlow, J.W., "Solid Freeform Fabrication Proceedings," University of Texas/Austin, Austin, Texas, (Aug. 1998).

[21] Mariotti, C., Manos, M.T., Roselli, L., "Demonstration and Characterization of Fully 3D Printed RF Structures," Microwave Symposium (MMS) 2015 IEEE 15th Mediterranean, pp. 1-4 (Dec. 2015).